10 Aug 2016

3D Printing of a Polymer Bioactive Glass Composite for Bone Repair

Caroline Murphy

Krishna C. R. Kolan

M. Long

Ming-Chuan Leu
Missouri University of Science and Technology, mleu@mst.edu

et. al. For a complete list of authors, see https://scholarsmine.mst.edu/mec_aereng_facwork/4311

Recommended Citation

C. Murphy et al., "3D Printing of a Polymer Bioactive Glass Composite for Bone Repair," *Proceedings of the 27th Annual International Solid Freeform Fabrication Symposium (2016, Austin, TX)*, pp. 1718-1731, University of Texas at Austin, Aug 2016.

Solid Freeform Fabrication 2016: Proceedings of the 27th Annual International Solid Freeform Fabrication Symposium – An Additive Manufacturing Conference
Reviewed Paper

3D PRINTING OF A POLYMER BIOACTIVE GLASS COMPOSITE FOR BONE REPAIR

C. Murphy[1], K.C.R. Kolan[1], M. Long[1], W. Li[1], M.C. Leu[1], J.A. Semon[2], and D.E. Day[3]
[1]Mechanical and Aerospace Engineering
[2]Biological Sciences
[3]Materials Science and Engineering
Missouri University of Science and Technology, Rolla, MO

Abstract

A major limitation of synthetic bone repair is insufficient vascularization of the interior region of the scaffold. In this study, we investigated the 3D printing of adipose derived mesenchymal stem cells (AD-MSCs) with polycaprolactone (PCL)/bioactive glass composite in a single process. This offered a three-dimensional environment for complex and dynamic interactions that govern the cell's behavior *in vivo*. Borate based bioactive (13-93B3) glass of different concentrations (10 to 50 weight %) was added to a mixture of PCL and organic solvent to make an extrudable paste. AD-MSCs suspended in Matrigel was extruded as droplets using a second syringe. Scaffolds measuring 10x10x1 mm^3 in overall dimensions with a filament width of ~500 µm and pore sizes ranging from 100 to 200 µm were fabricated. Strut formability dependence on paste viscosity, scaffold integrity, and printing parameters for droplets of AD-MSCs suspended in Matrigel were investigated.

1. Introduction

Bone defects, resulting from trauma, cancer, arthritis, infection, or congenital skeletal abnormalities, contribute to major surgeries performed every year. Autologous bone graft is still considered as the golden standard for most applications but creates donor site morbidity [1, 2]. Allografts avoid these issues but have limited availability, concerns over immunogenicity, and potential disease transmission [3]. Several types of materials, including biocompatible metals, bioceramics, and biopolymers are currently being investigated as candidates for synthetic grafts. Additive manufacturing of these materials has shown that complex and strong implants can be made to treat different regions of bone, including load-bearing bone [4-6]. However, engineered bone scaffolds have not been as successful as autologous grafts due to insufficient vascularization and reduced biomechanical function [7, 8].

Borate based bioactive glasses are biocompatible, osteoconductive, and angiogenic. In comparison to the more common silicate based bioactive glass, such as 45S5 or 13-93 glass, bioactive borate glass (13-93B3) has a higher reaction rate (5-10 times faster than silicate glasses); is more resorbable (60 to 70% wt. loss) in a few days to weeks; and is angiogenic, antimicrobial, and osteo stimulatory/conductive [9]. Controlling the size of the glass particles means the degradation rate of the glass can also be controlled to some extent. With the bioactive glass, there is also the potential use of dopants that could increase the positive biological effects, such as angiogenesis. In comparison, hydroxyapatite resorbs slowly and undergoes little conversion to bone-like material after implantation and provides no flexibility to tailor the material properties for the application. Biocompatible polymers such as polycaprolactone (PCL),

provide strength and elasticity to scaffolds. PCL is one of the most widely used materials in 3D printing for biomedical applications because of its low cost and excellent rheological and viscoelastic properties [10]. Though PCL has a slow degradation rate (>2 years compared to few months for poly(lactic acid)/poly(glycolic acid) copolymers), a composite scaffold of 13-93B3 and PCL may provide the benefits of both 13-93B3 glass and PCL materials.

Mesenchymal stem / progenitor cells (MSCs) have been used for cell therapy and in tissue engineering because of their ability to differentiate into multiple mesenchymal lineages *in vitro*, immune modulatory effects, and angiogenic capacity [11, 12]. MSCs have been isolated from several tissues, including the bone marrow (BM-MSCs), adipose tissue (AD-MSCs), and skin tissue [13-16]. The frequency of MSCs in adipose tissue is much higher than the more commonly studied source of bone marrow, yielding 100 to 500 times more cells per tissue volume [17, 18]. AD-MSCs have similar self-renewal abilities, common surface epitopes, growth kinetics, and cytokine expression profiles to BM-MSCs. With the addition of MSCs, the scaffold is expected to improve its biomechanical and biological properties in order to better repair the target tissue.

Recent research has focused on creating living or cell-laden grafts for tissue engineering [19-21]. In such techniques, cells or cell aggregates are dispersed, typically in a hydrogel, and then deposited layer-by-layer and solidified either by thermal or chemical processes to form a scaffold. Though such a scaffold holds promise in wound healing, drug delivery, and certain tissue engineering applications, bone repair requires a certain amount of mechanical integrity and controlled degradation of the scaffold which is difficult to accomplish. Traditionally, biopolymer scaffolds are fabricated using the fused deposition modeling process, where a polymer is melted and deposited thereby making it difficult to print cells alongside because of relatively high working temperatures [7]. In this study, we investigate the feasibility of printing a 3D scaffold using a two syringe system with a biopolymer/bioglass composite dissolved in an organic solvent as a scaffold material whilst simultaneously printing cells suspended in Matrigel, a gelatinous protein mixture representing basement membrane.

2. Materials and Methods

2.1 Preparation of PCL+bioactive glass composite

PCL (Sigma-Aldrich, St. Louis, MO) was dissolved in chloroform (Sigma-Aldrich, St. Louis, MO) in a covered glass container with the help of a stirrer at ~50°C. The weight percentage of PCL was varied from 1:1 to 5:4 (grams of PCL to mL of chloroform) to determine the best possible ratio for printing. An appropriate ratio was established by visually inspecting the paste and through filament extrusion using a digital syringe dispenser. Then, 13-93B3 borate bioactive glass (Mo-Sci Corporation, Rolla, MO) (nominal composition – 53% B_2O_3, 20% CaO, 12% K_2O, 6% Na_2O, 5% MgO, 4% P_2O_5 in weight percentage) of size less than ~20 µm was added to the PCL:chloroform mix in five different weight percentages in increments of 10, ranging from 10% to 50%. A magnetic stirrer was used to uniformly mix the composite paste and it was ensured that there was no glass particle precipitate before transferring the paste to a syringe. Each ratio was tested using a Loctite® digital syringe dispenser (Henkel North America, Rocky Hill, CT) at air pressures ranging from 10 to 50 psi with nozzle tips ranging from 110 to 500 µm.

2.2 Scaffold fabrication

The PCL/glass scaffold (10 mm x 10 mm) was printed with 0-90° orientation of the filaments in alternate layers, shown as schematic in Figure 1a. Printing was performed with an assembled DIY 3D printer (Geeetech, Prusa I3 A Pro) which was modified to have two syringes connected to digital syringe dispensers and are computer controlled. The 3D printer set-up is shown in Figure 1b. The printing parameters such as filament spacing, layer height, printing speed, etc. were identified based on visual inspection and optical microscopic images after a single layer extrusion. Printing parameters such as needle tip size (260 µm) and printing speed (~ 8 mm/s) were uniform for all paste concentrations. Parameters such as air pressure and filament overlap are correspondingly modified for different pastes. Samples of 3D printed scaffolds were sputter coated with gold/palladium (Au/Pd) for 60 s before performing scanning electron microscopy (SEM). SEM (Hitachi S-4700 FESEM, Hitachi Co., Tokyo, Japan) images were taken to evaluate the surface morphology of scaffolds and internal structure of the filaments.

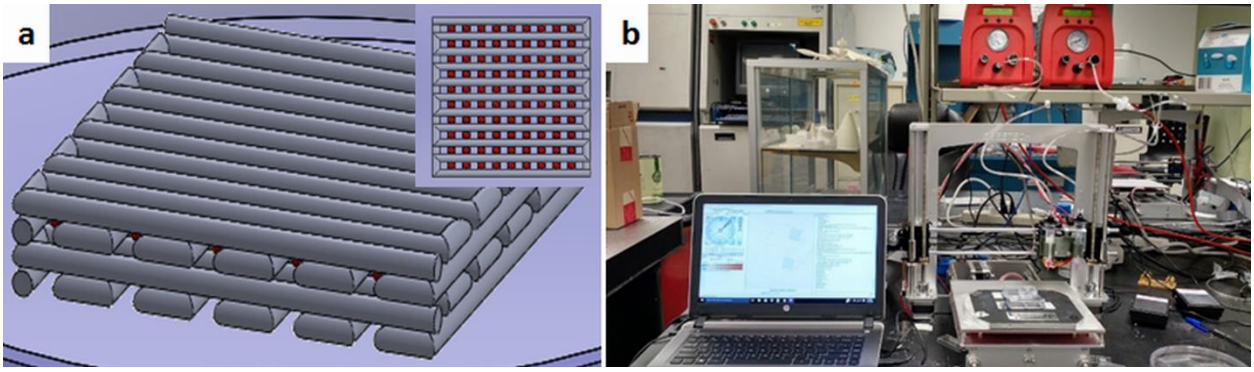

Figure 1. (a) Schematic showing the fabrication of PCL+Bioglass filaments in 0-90 layer orientation with cells suspended in Matrigel (red dots), (b) 3D printer set-up with digital syringe dispensers

2.3 Preparation and printing of AD-MSCs

Different concentrations of Matrigel, diluted in phosphate buffered saline (PBS), ranging from 4 mg/mL to 10 mg/mL were printed using 10 psi and a 160 µm (30G) diameter nozzle tip to determine the ideal concentration for printing with cells. Frozen vials of approximately $1x10^6$ AD-MSCs were obtained from three separate donors (LaCell, New Orleans, LA). Vials were unthawed, plated on 150 cm^2 culture dishes (Nunc, Rochester, NY) in 25 mL complete culture media (CCM), and incubated at 37.5^oC with 5% humidified CO_2. After 24 hours, the media was removed and adherent, viable cells were washed twice with PBS, harvested with 0.25% trypsin/ 1mM EDTA (Gibco), and replated at 100 cells/cm^2 in CCM. Media was changed every 3 to 4 days. For all experiments, sub-confluent cells (≤70% confluent) between passages 2 and 6 were used.

After determining that a concentration of 9 mg/mL Matrigel yielded the preferred droplet size, AD-MSCs at a concentration of $1x10^6$ cells/mL were suspended in Matrigel. The printing parameters for Matrigel+cells were tested by designing a blocked experiment with air pressure as the blocked variable (10 and 20 psi). The other two variables considered were extrusion time

(0.025 s and 0.035 s) and distance from the substrate (100 µm and 200 µm). A sample size of n = 3 was used for each droplet deposition with a specific set of parameters as shown in Table 1. When printing with Matrigel, the nozzle, cells, pipette tips, and Matrigel were all kept on ice until just before printing.

Table 1. Experimental set-up to determine the Matrigel+cell droplet parameters (n = 3)

Distance from substrate (µm)	Dispensing time (s)	Air pressure (psi)
100	0.025	10
200	0.025	10
100	0.035	10
200	0.035	10
100	0.025	20
200	0.025	20
100	0.035	20
200	0.035	20

2.4 Degradation of PCL+bioactive glass and AD-MSCs distribution in Matrigel

The degradation of the PCL/glass composite material was studied using a thin sheet of the composite prepared by pouring the PCL/glass mixture on a polished glass plate and tape casted using a doctor blade set at a thickness of 600 µm. The measured thickness of the dried film was 60±10 µm. Samples measuring 3 cm x 3 cm were cut from the sheet and kept in 50 mL of simulated body fluid (SBF) at 37°C. After the desired time intervals, the composite samples were removed from SBF and dried at 50°C for 12 h. The weight loss of each sample was measured and the SBF solution was analyzed by inductive coupled plasma spectroscopy (ICP) for boron, silicon, calcium, and phosphorus. To analyze the MSC distribution in Matrigel, 4',6-diamidino-2-phenylindole (DAPI) stain was used to image the Matrigel+cell droplets using fluorescent microscopy.

2.5 Effect of Chloroform Evaporation on AD-MSC Viability

The effect of chloroform evaporation from the scaffold on the viability of the AD-MSCs was studied by printing three layers of the 30% glass composite on a two chamber microscope slide (Thermo Fischer Scientific, Rochester, NY) then printing a layer of AD-MSCs at a concentration of $10x10^6$ cells per mL of Matrigel. The composite was printed according to the parameters given in Table 2 and the AD-MSCs were printed at 10 psi, 0.035 s dispensing time, and 200 µm from the slide. Four droplets of cells suspended in Matrigel, about 0.4 mm in diameter, were printed on each horizontal filament of the scaffold.

The Matrigel was allowed to polymerize at room temperature for 20 minutes then 1 mL of CCM was added. The slides were then incubated at 37.5^oC with 5% humidified CO_2. After 2 hours, the cells were stained according to the directions given with life technologies LIVE/DEAD Cell Imaging Kit (ref. R37601, Eugene, OR) and examined under a fluorescent scope. This was repeated again after 24 hours on a different set of scaffolds.

3. Results and Discussion

3.1 Fabrication of PCL+bioactive glass composite

Single layer tests: The weight percentage of PCL was varied from 1:1 to 5:4 (in grams of PCL to mL of chloroform) to determine the best ratio for fabricating the scaffold. During the initial set of tests, different compositions of paste were extruded using a hand-held syringe and with the help of a digital dispenser by varying the nozzle tip and air pressure. An air pressure between 30 and 50 psi provided uniform extrusion of the PCL+chloroform mixture. The ideal ratio of PCL and chloroform was determined to be 5 g of PCL to 3 mL of chloroform, extruded at 30 psi using a 260 µm (25G) nozzle tip. A larger tip size (>260 µm) would result in thick filaments which are considered not beneficial for achieving faster scaffold degradation and smaller pore size distribution in the scaffold. Afterwards, 10% 13-93B3 glass by weight was added to the PCL+chloroform mixture and then extruded with the same set of parameters without difficulty. Figure 2a to 2c shows the filament extrusion tests performed on a microscopic glass slide with varying printing speeds. A reduced filament width (from 1.8 mm to 0.8 mm) can be observed with increasing table speed, which was tested from 3 to 10 mm/s. The filament width is also dependent upon the homogeneity of the mixture. Figure 2d shows a successful and continuous single layer of a 15 cm x 15 cm scaffold with the filament spacing of 0.7 mm and a printing speed of 8 mm/s.

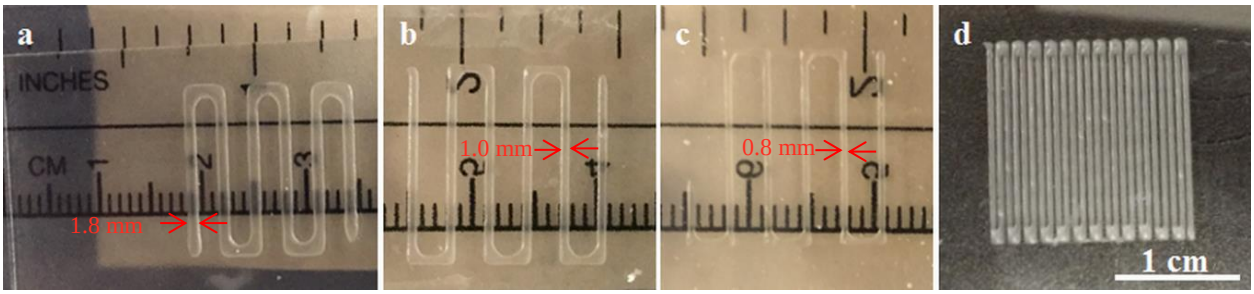

Figure 2. Single layer tests with (PCL+10% Glass) and different printing speeds (a) 3 mm/s, (b) 5 mm/s, (c) 10 mm/s, and (d) 8 mm/s (which is used for rest of the experiments).

Two layer tests: The filament height and spacing of the first layer would be crucial parameters to print successive layers. Filament height would determine the layer height and filament spacing would define how well the bridging occurs in successive layers. Figure 3a shows the optical microscopic image of the cross-sections of the first layer filaments. The average height of the filament (shown between the two arrows) was ~75 µm. The height of the filaments for 40 wt% and 50 wt% compositions remained the same as long as the same nozzle tip was used. The roundness of the filament improved with a smaller tip but because of the nozzle clogging issues, all the experiments were carried out with a 260 µm tip. Therefore, a layer height of 0.08 mm was used to fabricate subsequent scaffolds. Another important factor in this study is the dwell time between consecutive layers as this allows the chloroform to evaporate thereby allowing the previous layer to become dry. A longer dwell time (>5 min) would warp the layer and a shorter dwell time (<1 min) is not sufficient for the layer to dry. Figures 3b and 3c show the results of printing a second layer with no dwell time and with 1 min dwell time, respectively, with a 0.8 mm filament spacing. The difficulty in bridging the second layer without dwell time

can be noticed, which was substantially improved with 1 mm dwell time. Figure 3d shows the bridging of second layer with 2.5 min of dwell time and 0.7 mm filament spacing.

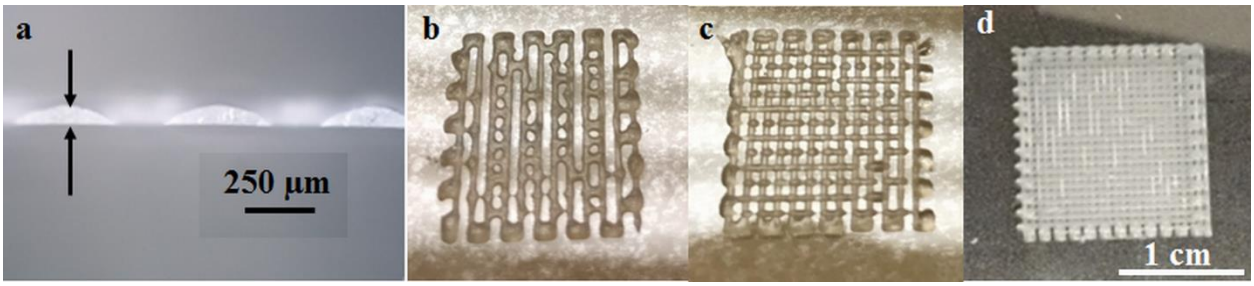

Figure 3. (a) Cross-sectional view of the PCL/glass filament measuring ~75 µm in height, (b) second layer printing with zero dwell time, (c) second layer printing with 1 min dwell time, and (d) second layer printed on top of the layer shown in Figure 2d with 2.5 min dwell time

Multiple layer scaffolds: Based on the best printing parameters determined, scaffolds with multiple layers were fabricated with all five PCL/glass compositions (10 to 50 weight percentage of 13-93B3 glass). For compositions made with 40 wt% and 50 wt% glass, the amount of chloroform required to obtain a pourable characteristic for the paste was 4 mL (instead of 3 mL to 5 g of PCL). This is believed to be due to the increased viscosity of the paste with increase in glass content. With the exception of the paste made with 30 wt% of glass, which was extruded at an air pressure of 40 psi, remaining paste compositions were extruded at an air pressure of 30 psi. The final set of parameters used to fabricate scaffolds is given in Table 2. The filament width of 500±50 µm was measured for all compositions printed with a 260 µm nozzle tip while the average pore size depended on the filament spacing. A spacing of 0.6 mm provided pore sizes ranging from ~100 to ~200 µm while in scaffolds with a spacing of 0.7 mm, the pore size varied from ~200 to ~300 µm. Figure 4a shows an optical microscopic image of a scaffold fabricated with a filament spacing of 0.6 mm and with a smaller pore size distribution. As can be seen, pore sizes could be adjusted by modifying the filament spacing, to a certain extent, to suit a certain tissue engineering application of the fabricated scaffold. It is known that pore size is an important aspect of the scaffolds that could potentially effect the bone growth after implantation and it has been reported that pore sizes in the range of 100 to 300 µm are beneficial for bone growth [8]. The scaffolds fabricated by our process have pores in the same range. Figure 4b shows images of 10 mm x 10 mm scaffolds fabricated with 0.8 mm spacing.

Table 2. Final printing parameters for each of five PCL/glass paste compositions

13-93B3 Glass (Wt. %)	Air Pressure (psi)	PCL:Chloroform (g to mL)	Filament Spacing (mm)
10	30	5:3	0.6 – 0.8
20	30	5:3	0.6 – 0.8
30	40	5:3	0.6 – 0.8
40	30	5:4	0.7 – 0.9
50	30	5:4	0.7 – 0.9

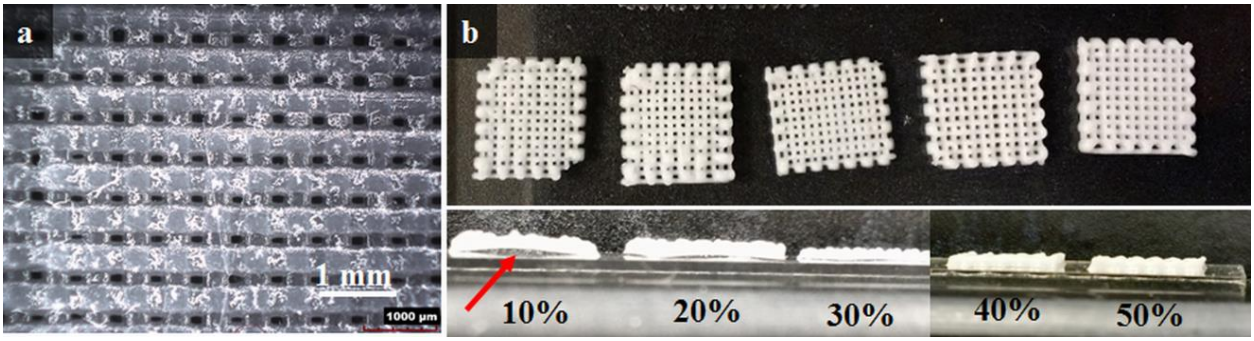

Figure 4. (a) Optical microscopic image showing the pore size distribution (~150 µm) in a scaffold fabricated with 0.6 mm filament spacing, (b) (L-R) pictures of representative scaffolds made with 10% to 50% glass content; the bottom image shows the warpage of scaffolds containing 10 to 30 wt.% glass with the red arrow indicating the space between the scaffold and slide. No warpage is seen in 40% and 50% scaffolds; scaffold with 50 wt% glass is the thickest fabricated (1 mm).

It should be noted that the maximum thickness (or height) of the scaffolds depends on the degree of chloroform evaporation and the distance between layers. All of our experiments were carried out at room temperature (64°F) where the variation in relative humidity (58-60%) was not considered to be a major factor. Faster chloroform evaporation would produce warpage of the fabricated scaffold, especially with some dwell time between the layers. Non-uniform distribution of the PCL and glass is not believed to be one of the major factors of warpage as, upon examination of the filaments' microstructure when printed with the same syringe at different time intervals, there was similar and uniform deposition of glass particles throughout the matrix. Therefore, the chloroform evaporation and the percentage of PCL in the composite is one of the crucial factors which determines the warpage. Increasing the glass content in the composite would indirectly decrease the chloroform content and thereby aids in faster evaporation and improves the filament rigidity. In this study, it was observed that after reaching a thickness of about 0.64 mm (8 layers), the scaffolds being fabricated with 10% and 20% glass exhibited warping which led to difficulty in printing successive layers (see Figure 4b). The warpage in scaffolds made with 30% and 40% glass was less pronounced and thickness of 0.8 mm (10 layers) was obtained. The best results were achieved for 50% glass scaffolds as they were successfully printed to 1 mm thickness (12 layers) and could possibly have successive layers printed. Larger thicknesses were not attempted as the focus of this study is on the feasibility of printing PCL/glass scaffold along with MSCs. Though the mechanical properties of the scaffolds are not measured, it was observed that the ease of handling scaffolds improved with increasing glass content. The scaffold made with 50% glass had enough strength to be safely handled.

Microstructure of PCL/glass composite scaffolds: Figure 5 shows the scanning electron micrographs of a couple of representative PCL/glass scaffolds made with 40 and 50 wt.% glass. Figures 5a to 5c show the surface morphology of the filament with increasing magnification (x30, x90, and x2000). It was interesting to observe that particles of bioglass are conspicuously absent from the surface of filaments. No pores on the filament surface were detected even when observed at a high magnification of x2000. Figures 5d to 5e show the filament fracture surface with increasing magnification (x180, x1000, and x2000). Glass particles dispersed in the PCL matrix can be seen in the interior. The dissolved PCL in chloroform encloses the glass particles

and the surface tension effects between the steel nozzle tip and PCL during extrusion might cause the presence of only PCL on the surface.

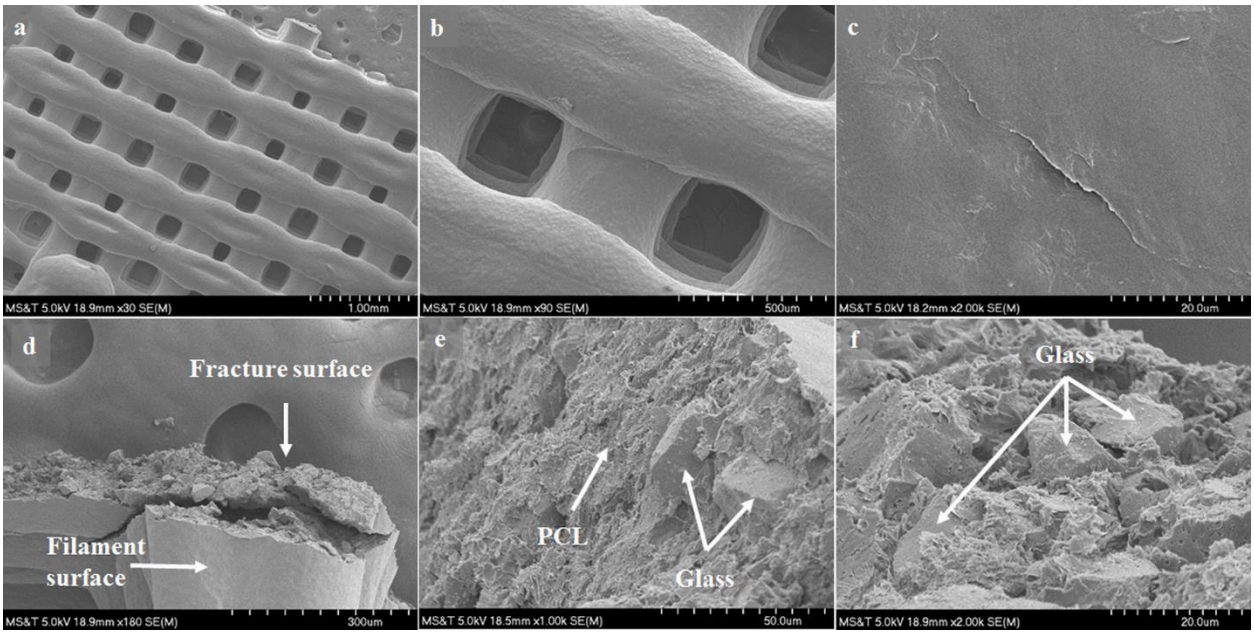

Figure 5. SEM images of the PCL/glass scaffolds. (a-c) Images with increased magnification from L-R showing a smooth surface morphology of the filament (40% glass scaffold), (d-f) Images with increased magnification from L-R (50% glass scaffold) (d) showing the fracture surface, (e-f) porous cross-sectional area of the filament with PCL matrix and glass particles

3.2 Degradation of PCL+bioactive glass composite in Simulate Body Fluid

A "PCL+13-93B3 glass+chloroform" composite system has been studied in the recent past by producing thin sheets (60±10 µm) of PCL/glass composite [22]. The 3 cm x 3 cm sheet samples were soaked in SBF, dried overnight and weighed to measure their weight loss. The results indicate that 13-93B3 glass in the PCL/glass sheet had fully reacted to form hydroxyapatite (HA) in about 3 days. Figure 6 shows the weight loss percentages of the composite sheets made with different glass contents (20B – 20 wt.%, 40B – 40 wt.%, and 50B – 50 wt.% of 13-93B3 glass). In all three composites, reaction of the borate glass occurred rapidly during the first three to six days and then weight loss remains nearly constant. As expected, there was no loss of weight after 14 days for PCL. Also, weight loss increases with the increasing weight percentage of borate glass. The arrows on the right axis indicate the ideal weight loss for each composite which is weight loss of the glass if it completely reacted in SBF to form stoichiometric HA ($Ca_{10}(PO_4)_6(OH)_2$). A similar degradation profile for 3D printed composite scaffolds with different glass compositions is expected.

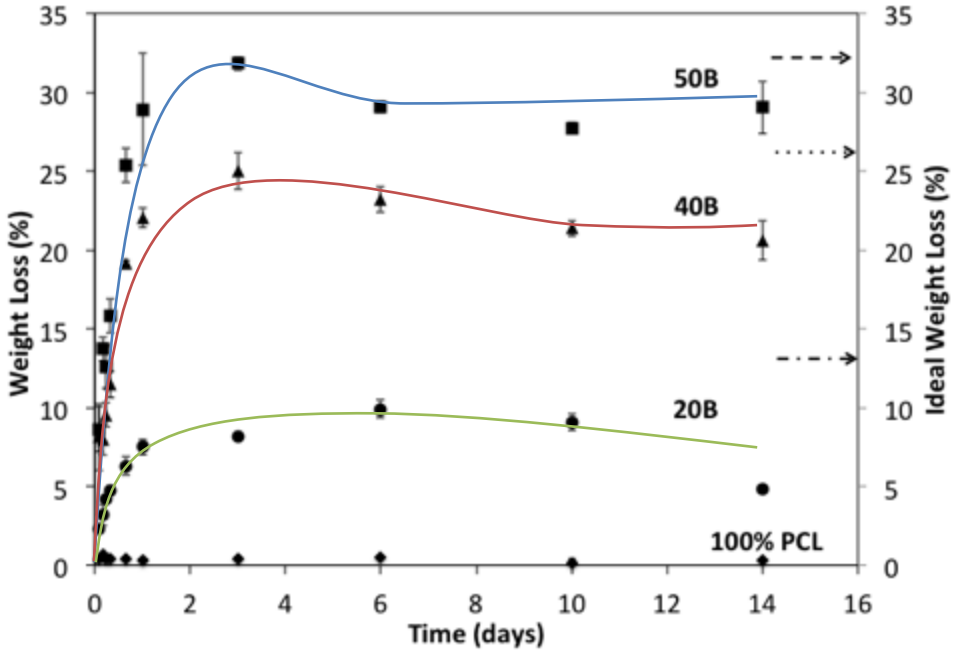

Figure 6. Weight loss for 50%, 40% and 20% glass compositions w.r.t weight loss of 100% PCL. The arrows on the right indicate the ideal weight loss for each composite [22].

3.3 Dispensing AD-MSCs suspended in Matrigel

Experiments were conducted to print droplets of Dulbecco's Modified Eagle Medium (DMEM) which contained suspended AD-MSCs. It was determined that a 110 µm (32G) nozzle tip extruded droplets less than 500 µm suitable for printing either on top or alongside the deposited PCL/glass filaments. However, the DMEM in the printed droplets would evaporate quickly making it difficult for further investigation. Therefore, the option of using Matrigel as the medium to suspend the MSCs was considered. The initial set of experiments included dispensing the Matrigel droplets without cells with the syringe dispensing system set-up to determine an appropriate concentration of Matrigel and droplet size. A concentration of 10 mg/mL Matrigel provided smaller drops (~100 µm), while 8 mg/mL Matrigel produced larger drops (~500 µm), and 4 mg/mL Matrigel produced even larger drops (1 mm). In each case, Matrigel provided a stable environment for the cells without drying (measured for up to 10 minutes). As the filament width of the scaffolds was measured between 400 to 500 µm, a Matrigel concentration of 9 mg/mL was selected to be appropriate for generating droplets which could be deposited on top of the filaments. Approximately $1x10^6$ cells suspended in PBS were pipetted in Matrigel. The AD-MSCs+Matrigel solution was then transferred just before printing to a 160 µm nozzle tip which was stored on ice during the entire non-printing time. It is assumed that the MSCs were uniformly distributed in the Matrigel before the start of the droplet deposition.

An experiment was conducted to dispense Matrigel droplets with suspended MSCs by varying parameters including distance of the nozzle tip from glass slide, dispensing time of droplet, and air pressure. ImageJ software was utilized to quantify the number of cells in each fluorescent image. Figure 6 shows DAPI stained images of Matrigel droplets with $1x10^6$ cells/mL printed at different parameters. Figures 7a-7d show the fluorescent images of the

Matrigel droplets printed with 10 psi air pressure and Figures 7e-7h show the Matrigel droplet images printed with 20 psi air pressure. It can be clearly observed that droplets made at higher air pressure have a blue ring (cells are identified by blue dots in Figure 7) indicating that cells are at the boundary of the droplet because of the high pressure. This result is irrespective of the other two parameters. Droplets printed at the low air pressure (10 psi) have a smaller diameter and provide a more uniform distribution of cells. Such a distribution would be beneficial and the droplet size (<500 µm) would be appropriate to print on the PCL/glass filament. Among the four sets of droplets printed with 10 psi, it is observed that those printed with a distance offset of 200 µm had more cells (150 and 153) in comparison to those printed with an offset of 100 µm (105 and 148). Further, amongst the droplets printed with 200 µm offset distance and 10 psi pressure, the droplets printed with a pulse time of 0.035 s was measured to have slightly higher cell count (153) in comparison to those printed at 0.025 s (150). These results allow us to determine the printing parameters for depositing Matrigel droplets, which are: (i) air pressure of 10 psi, (ii) distance from glass slide of 200 µm, and (iii) pulse duration of 0.035 s. Figure 6a shows a Matrigel droplet printed with the above set of parameters. Select cells are marked using arrows for better comprehension of the image in print. Investigating the cell survivability on the "PCL+13-93B3 glass+chloroform" filament is a crucial step toward our goal of establishing a novel and successful method of 3D printing of scaffolds with living cells for tissue engineering.

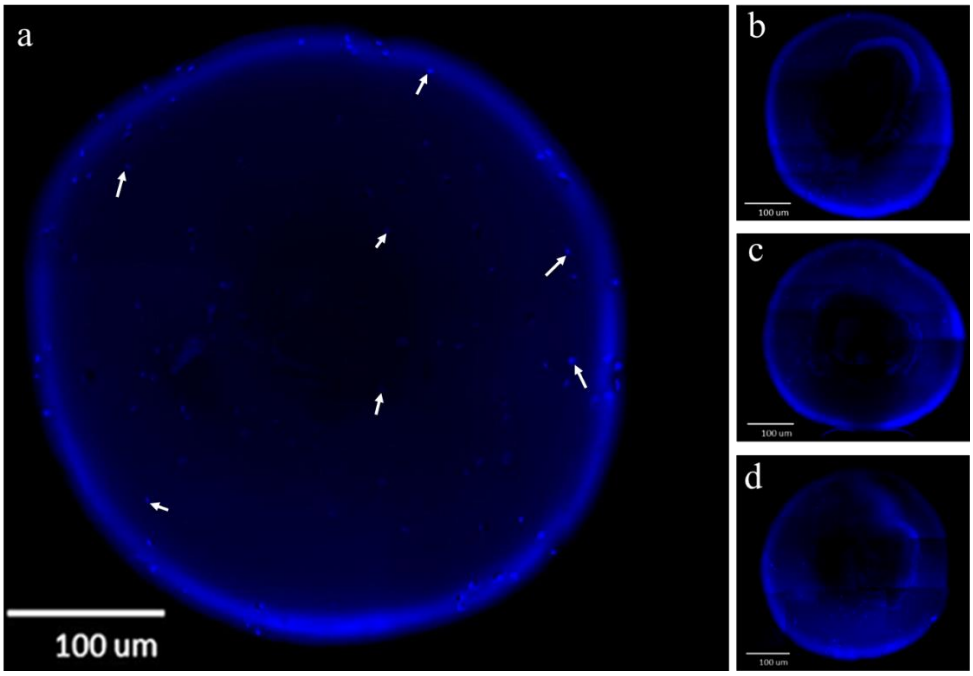

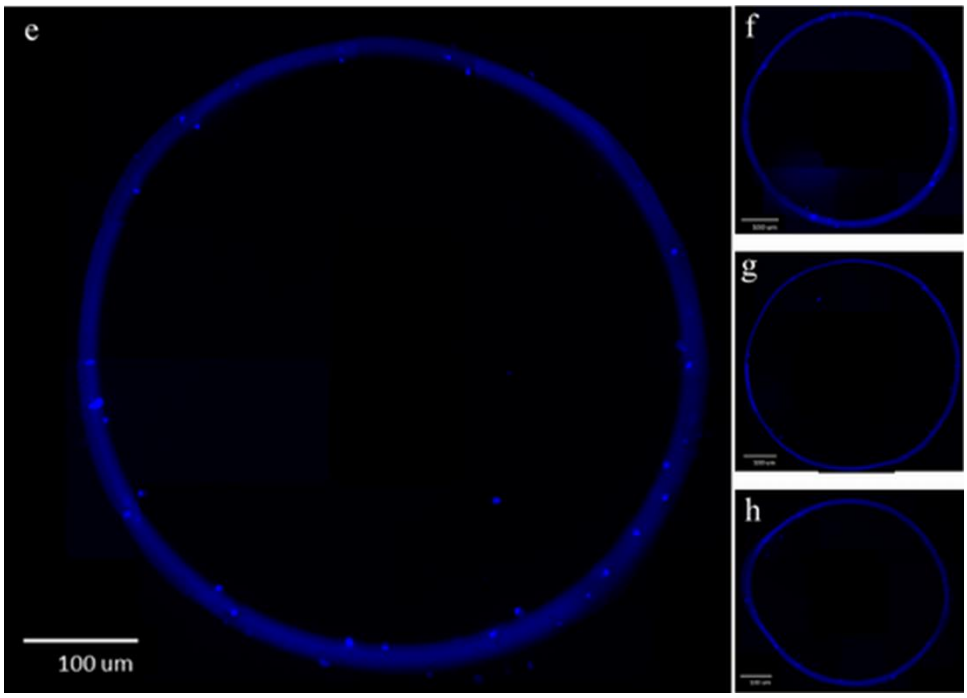

Figure 7. DAPI stained fluorescent images of AD-MSC/Matrigel droplets, printed at (a-d) 10 psi and (e-h) 20 psi air pressure. (a) A pulse time of 0.035 s and 200 µm distance from glass slide (b) 0.025 s and 200 µm (c) 0.035 s and 100 µm (d) 0.025 s and 100 µm. The cells are at the boundary of the droplet because of higher air pressure.

3.4 Effect of Chloroform Evaporation on AD-MSC Viability

Viability of AD-MSC after printing was determined by a live/dead assay 2 and 24 hours after printing (Figure 8). At two hours, 96% were viable, demonstrating a minimal negative effect on the cells shortly after printing. At 24 hours, 65% were viable, indicating the potential for long term growth of the cells.

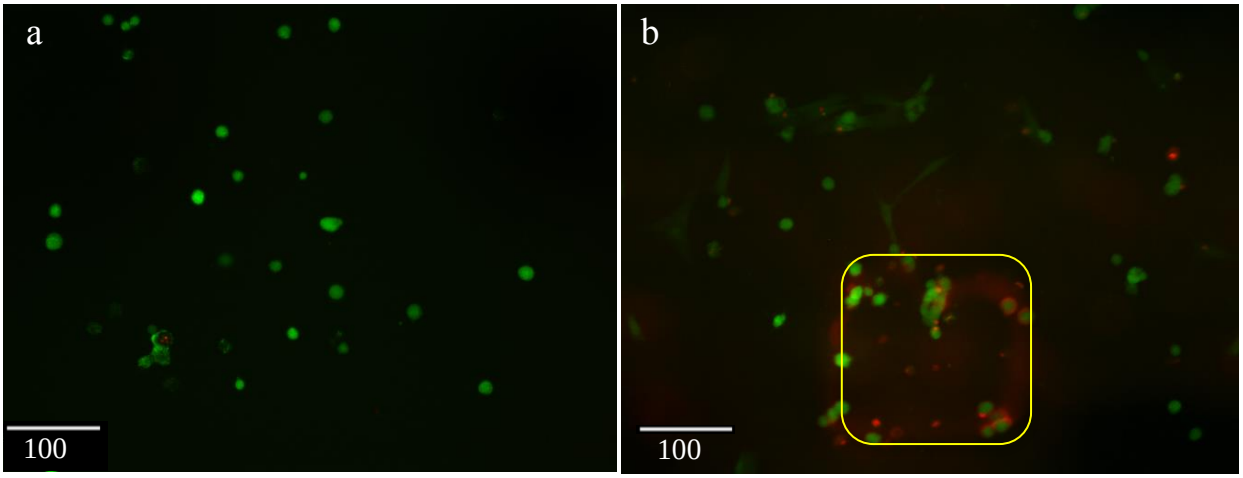

Figure 8. Live/Dead images of AD-MSC/Matrigel droplets printed on 3 layers of the 30% glass PCL composite. Imaged after (a) 2 hours and (b) 24 hours. The yellow square indicates a pore in the scaffold.

4. Conclusion

This study investigated the feasibility of fabricating a scaffold with polycaprolactone (PCL) and 13-93B3 bioactive borate glass composite utilizing a 3D printer without any heat input. This method would allow the process to incorporate cells during the printing of a scaffold unlike other processes where heating of the biopolymer is involved. Scaffolds were printed and near optimal printing parameters for each of the five different PCL/glass compositions were determined. Scaffolds fabricated with a 50:50 (in weight percentage) PCL/glass composite utilizing the parameters of 30 psi, 5 g of PCL to 4 mL of chloroform, 0.8 mm filament spacing were easy to handle with sufficient mechanical integrity. Printing parameters for depositing cells suspended in Matrigel were determined and uniform distribution of cells in a ~400 μm droplet size was obtained for an air pressure of 10 psi and 0.035 s pulse. A live/dead assay performed 2 and 24 hours after printing cells on a 3 layer scaffold showed minimal negative effects from chloroform evaporation on the cells. The results of this study show the potential of the process to fabricate a scaffold with living cells embedded for tissue engineering applications.

A continuation of this study would include increasing the height of the scaffold. To achieve this, the scaffold fabrication process will be modified by avoiding the continuous printing of the single layer and incorporating start-stop operations to deposit each filament in the layer. Such an operation would avoid the excess build-up of material at the scaffold edge which aids in building thicker scaffolds. The objective of this study is to simultaneously print the MSCs and PCL+glass. Therefore, the viability of printing MSCs based on the height of the scaffold will also be investigated. The degradation of the PCL+glass scaffolds is a work in progress and despite its known hydrophobicity, the initial results indicate that DI water/cell culture media is able to penetrate PCL and helps in glass dissolution. In this context, it is believed that the fabricated scaffolds tend to be more porous than the designed porosity of ~50%. Further experiments will be performed to investigate the overall scaffold porosity. In relation to cell viability, a live/dead assay will be performed for 24 hours, 1 week, and 2 weeks with the 50% glass composition.

Acknowledgment

The 13-93B3 glass used in this study was provided by MO-SCI Corporation, Rolla, MO. The authors thank Wenbin Li for his help in setting up the printer and Mariahe Long for her help with imaging.

References

1. J.C. Banwart, M.A. Asher, and R.S. Hassanein, “Iliac crest bone graft harvest donor site morbidity: A statistical evaluation,” *Spine*, 20 [9] 1055-1066, 1995.
2. J.A. Goulet, L.E. Senunas, G.L. DeSilva, and M.L.V.H. Greenfield, “Autogenous iliac crest bone graft: Complications and functional assessment,” *Clinical orthopaedics and Related Research*, 339 76-81, 1997.
3. P.B. Giannoudis, H. Dinopoulos, and E. Tsiridis, “Bone substitutes: an update,” *Injury*, 36 [3] S20-27, 2005.

4. N.D. Doiphode, T. Huang, M.C. Leu, M.N. Rahaman, and D.E. Day, "Freeze extrusion fabrication of 13–93 bioactive glass scaffolds for bone repair," *J. Mater Sci: Materials in Medicine*, 22 [3] 515-523, 2011.
5. K.C. Kolan, M.C. Leu, G.E. Hilmas, and M. Velez, "Effect of material, process parameters, and simulated body fluids on mechanical properties of 13-93 bioactive glass porous constructs made by selective laser sintering," *Journal of the Mechanical Behavior of Biomedical Materials*, 1314-24, 2012.
6. P. Bartolo, J.P. Kruth, J. Silva, G. Levy, A. Malshe, K. Rajurkar, and M. Leu, "Biomedical production of implants by additive electro-chemical and physical processes," *CIRP Annals - Manufacturing Technology*, 61 [2] 635-655, 2012.
7. J.P. Temple, D.L. Hutton, B.P. Hung, P.Y. Huri, C.A. Cook, R. Kondragunta, X. Jia, and W.L. Grayson, "Engineering anatomically shaped vascularized bone grafts with hASCs and 3D-printed PCL scaffolds," *J. Biomed Mater Res A*, 102 [12] 4317-4325, 2014.
8. M.N. Rahaman, D.E. Day, S. Bal, Q. Fu, S.B. Jung, L.F. Bonewald, and A.P. Tomsia, "Bioactive glass in tissue engineering," *Acta Biomater.*, 7[6] 2355-2373, 2011.
9. Y. Lin, R.F. Brown, S.B. Jung, and D.E. Day, "Angiogenic effects of borate glass microfibers in a rodent model," *J Biomed Mater Res* A, 102 [12] 4491-4499, 2014.
10. I. Armentano, M. Dottori, E. Fortunati, S. Mattioli, and J.M. Kenny, "Biodegradable polymer matrix nanocomposites for tissue engineering: a review," *Polymer Degradation and Stability*, 96 [11] 2126-2146, 2010.
11. H.K. Salem and C. Thiemermann, "Mesenchymal stromal cells: Current understanding and clinical status," *Stem Cells*, 28 [3] 585-596, 2010.
12. Y. Wu, L. Chen, P.G. Scott, and E.E. Tredget, "Mesenchymal stem cells enhance wound healing through differentiation and angiogenesis," *Stem Cells*, 24 [10] 2648-2659, 2007.
13. D.A. De Ugarte, K. Morizono, A. Elbarbary, Z. Alfonso, P.A. Zuk, M. Zhu, J.L. Dragoo, P. Ashijian, B. Thomas, P. Benhaim, I. Chen, J. Fraser, and M.H. Hedrick, "Comparison of multi-lineage cells from human adipose tissue and bone marrow," *Cells Tissues Organs*, 174 [3] 101-109, 2003.
14. R. Izadpanah, C. Trygg, B. Patel, C. Kriedt, J. Dufour, J.M. Gimble, and B.A. Bunnell, "Biologic properties of mesenchymal stem cells derived from bone marrow and adipose tissue, " *J Cell Biochem*, 99 [5] 1285-1297, 2006.
15. W. Wagner, F. Wein, A. Seckinger, M. Frankhauser, U. Wirkner, U. Krause, J. Blake, C. Schwager, B. Eckstein, W. Ansorge, and A.D. Ho, "Comparative characteristics of mesenchymal stem cells from human bone marrow, adipose tissue and umbilical cord blood," *Exp Hematol*, 33 [11] 1402-1416, 2005.
16. Y. Sakaguchi, I. Sekiya, K. Yagishita, and T. Muneta, "Comparison of human stem cells derived from various mesenchymal tissues: superiority of synovium as a cell source," *Arthritis Rheum*, 52 [8] 2521-2529, 2005.
17. F. D'Andrea, F. De Francesco, G.A. Ferraro, V. Desiderio, V. Tirino, A. De Rosa, and G. Papaccio, "Large-scale production of human adipose tissue from stem cells: a new tool for regenerative medicine and tissue banking," *Tissue Eng Part C Methods*, 14 [3] 233-242, 2008.
18. L. Casteilla and C. Dani, "Adipose tissue-derived cells: from physiology to regenerative medicine," *Diabetes Metab*, 32 [5] 393-401, 2006.

19. T.K. Merceron, M. Burt, Y.J. Seol, H.W. Kang, S.J. Lee, J.J. Yoo, and A. Atala, "A 3D bioprinted complex structure for engineering the muscle-tendon unit," *Biofabrication,* 7 [3] 2015.
20. B. Duan, L.A. Hockaday, K.H. Kang, and J.T. Butcher, "3D bioprinting of heterogenous aortic valve conduits with alginate/gelatin hydrogels," *J. Biomed Mater Res A,* 101 [5] 1255-2364, 2013.
21. Z. Wu, X. Su, Y. Xu, B. Kong, W. Sun, and S. Mi, "Bioprinting three-dimensional cell-laden tissue constructs with controllable degradation," *Scientific Reports,* 6 24474, 2016.
22. A. Mohammadkhah, L.M. Marquardt, S.E. Sakiyama-Elbert, D.E. Day, and A.B. Harkins, "Fabrication and characterization of polycaprolcatone and bioactive glass composites for tissue engineering applications," *Mater Sci Engr: C,* 49 [1] 632-639, 2015.